Journal of Plant Diseases and Protection (2026) 133:113
https://doi.org/10.1007/s41348-026-01303-5

ORIGINAL ARTICLE

Exploring the antifungal potential of *Lignosus rhinocerus* as a green nano factory for silver nanoparticles synthesis against plant pathogens

Muhammad Shahbaz[1] · Chuan Cheak Chong[1] · Kishneth Palaniveloo[2,3] · Jaya Seelan Sathiya Seelan[1]

Received: 17 December 2025 / Accepted: 1 June 2026

Abstract

Fungal pathogens including *Fusarium* and *Aspergillus* species are harmful to agricultural crops and are becoming increasingly resistant to existing antifungal drugs. Therefore, it is necessary to explore safer and more effective alternatives. *Lignosus rhinocerus* (LR), a medicinal mushroom rich in bioactive metabolites, provides an environmentally sustainable source of reducing and stabilizing agents for the synthesis of silver nanoparticles (AgNPs). In this study, *L. rhinocerus* extract was used for the synthesis of silver nanoparticles (AgNPs). The gradual change in color of the reaction mixture from light to dark brown indicated that Ag^{+} ions were reduced. This was further confirmed throughultraviolet (UV)-visible (VIS) spectroscopy, which showed an absorption peak at 410 nm. Scanning electron microscopy (SEM), revealedthat most of the *L. rhinocerus*-mediated silver nanoparticles (LR-AgNPs) were spherical to slightly irregular in shape. The particle sizes ranged from 60 to 85 nm. Energy-dispersive X-ray (EDX) analysis confirmed the successful synthesis of LR-AgNPs, showing a strong silver peak in elemental form along with other elements such as aluminium (Al), iron (Fe), and oxygen (O). Different functional groups (O–H, N–H, aliphatic C–H, amide I and II, C–N, C–O, and C–O–C) were identified using Fourier transform infrared spectroscopy (FTIR). The dynamic light scattering (DLS) exhibited a particle size distribution with a dominant peak cantered at approximately ~ 100 nm, within a size range of ~ 80–120 nm. To test the antifungal activities of LR-AgNPs, various concentrations (100–500 ppm) of LR-AgNPs and antifungal drug Fluconazole (FLZ) were applied against *Fusarium solani* and *Aspergillus ochraceus* using the well diffusion assay. The results revealed that LR-AgNPs effectively suppressed the growth of *F. solani* and *A. ochraceus*, producing zones of inhibition of 33.0 mm and 16.0 mm, respectively, at a concentration of 500 ppm. Furthermore, a radial growth assay conducted at 500 ppm demonstrated that LR-AgNPs inhibited the growth of *F. solani* by 76% and *A. ochraceus* by 61%. To the best of our knowledge, this is the first study that described the synthesis of silver nanoparticles (AgNPs) from *L. rhinocerus* extract. Future work should explore their mechanisms, safety, and formulation to advance practical applications.

✉ Jaya Seelan Sathiya Seelan
seelan80@ums.edu.my

[1] Institute for Tropical Biology and Conservation (ITBC), Universiti Malaysia Sabah, Jalan UMS, 88400 Kota Kinabalu, Sabah, Malaysia

[2] Institute Ocean and Earth Sciences, Universiti Malaya, 50603 Kuala Lumpur, Malaysia

[3] Centre for Natural Products Research and Drug Discovery (CENAR), Level 3, Research Management & Innovation Complex, Universiti Malaya, Wilayah Persekutuan, 50603 Kuala Lumpur, Malaysia

Published online: 03 July 2026

Graphical abstract

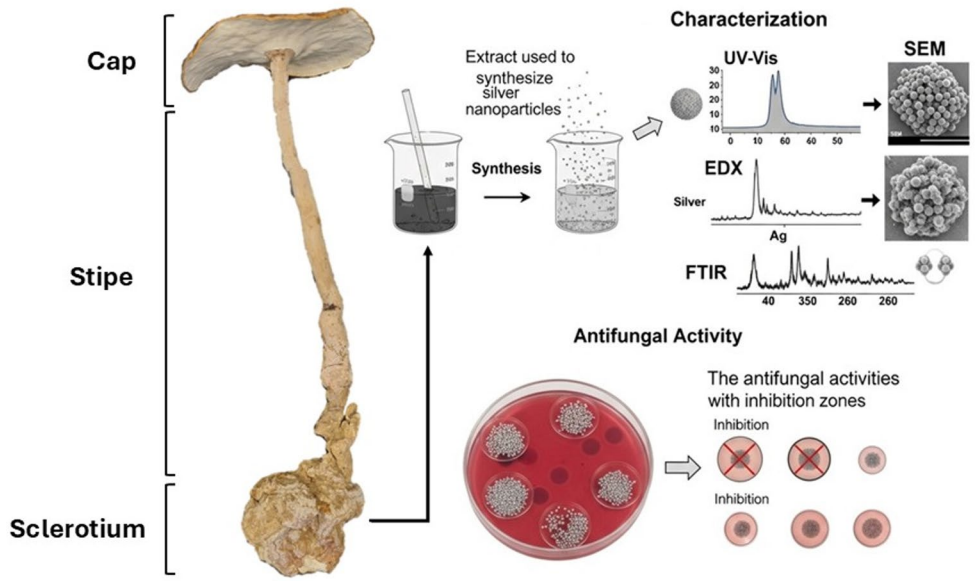

Keywords Bio-compatible · Bio-fabrication · Eco-friendly · Nanobiotechnology · And tiger milk mushroom

Introduction

Fungal diseases represent a major challenge to the global agricultural sector, leading to substantial annual economic losses (Nizamani et al. 2024; Tripathi et al. 2024; Tian et al. 2020). Plant diseases caused by fungal pathogens cost the world economy about $220 billion annually and result in a 20–40% loss in crop production (Nizamani et al. 2024; Li et al. 2017). *Fusarium* species are among the most damaging plant pathogens in agriculture and can infect many tropical crops worldwide (Dean et al. 2012). *Fusarium solani* affects important crops such as tomato, soybean, pea, and potato, causing root rot and wilt diseases, while *Aspergillus ochraceus* is associated with contamination of cereals, coffee, and stored grains, leading to both yield losses and mycotoxin production (Chen et al. 2025; Waghmode and Samudra 2025; Tiwari et al. 2024; Šišić et al. 2025; Hagos et al. 2024).They can function as saprophytes or pathogens, infecting both above-ground and below-ground parts of plants, either as primary or secondary pathogens (Summerell et al. 2003). The genus includes at least 300 species that are not closely related to each other; 20 species complexes and nine monotypic lineages have been identified so far (O'Donnell et al. 2015). Most *Fusarium* species live in soil, but *Fusarium* conidia can be spread by water through rain splashes and irrigation systems. When dry, they become airborne, which allows them to spread over long distances worldwide and employ a variety of infection strategies**.** These fungi are classified as hemibiotrophs, with the ability to shift to a necrotrophic lifestyle in response to environmental and metabolic signals (Fernando et al. 2000; Perfect and Green 2001). The agriculture sector is increasingly compelled to develop and adopt innovative, sustainable and targeted strategies to combat infections, especially *Fusarium* species, which have widespread distribution, diverse infection strategies, and cause substantial economic losses (Blakeney 2022; Desai et al. 2020).

Nowadays, nanotechnology is becoming increasingly applied in modern farming, providing new ways to deal with problems caused by fungal plant diseases and to improve overall agricultural productivity. The antifungal properties of metals, metal oxides, bio-nanoparticles, and polymer nanoparticles have been extensively investigated (Zhou et al. 2023; Nizamani et al. 2024). The traditional way to make silver nanoparticles (AgNPs) using physicochemical methods requires high energy, involves toxic chemicals, and contributes to environmental pollution (Fatima et al. 2016). In response, green chemistry via biosynthesis enables the production of biocompatible AgNPs using the metabolic processes of living organisms, especially fungi. Mycosynthesis is an environmentally friendly approach that uses fungi as efficient ""nanofactories." and represents a more sustainable approach compared to traditional methods (Beltrán Pineda et al. 2023; Manimaran et al. 2023).

Lignosus rhinocerus, commonly known as the tiger milk mushroom, is a unique medicinal mushroom with significant bioactive properties, classified within the Polyporaceae family and indigenous to Malaysia (Lee et al. 2011; Fung et al.

2022). About 400 years ago, "The Diary of John Evelyn" was the first book to mention the tiger milk mushroom (TMM; *Lignosus rhinocerus*). An important medical product, it is locally known as "cendawan susu rimau" or "kulat susu rimau," which means "Tiger Milk mushroom." TMM was successfully cultivated in 2009, leading to its commercial availability and the initiation of research into its therapeutic applications (Evelyn 1994). Researchers have shown that its sclerotium extracts can exhibit anti-inflammatory, anti-asthmatic, and antibacterial activities, as well as immune-boosting properties (Lau et al. 2014; Kamal et al. 2023; Lee et al. 2014; Johnathan et al. 2016; Wong et al. 2011). Earlier studies indicated that only selenium and gold nanoparticles had been synthesized using *Lignosus rhinocerus* (Cai et al. 2018; Azlan et al. 2020). *Lignosus rhinocerus* extracts have recently been shown to convert gold ions into AuNPs (Katas et al. 2019). There are many reports on the medicinal and bioactive properties of *L. rhinocerus*, but the synthesis of silver nanoparticles and their antifungal properties are still not well known. Although, several studies have reported fungal-mediated synthesis of AgNPs, studies using *L. rhinocerus* remain limited. To the best of our knowledge, the current research work is the first investigation of mycosynthesis of silver nanoparticles mediated by *L. rhinocerus* (LR-AgNPs) and their antifungal properties. The study underscores the potential of *L. rhinocerus* as an innovative biological source for the green synthesis of AgNPs and illustrates the antifungal effectivenessanti- of LR-AgNPs, thereby offering new perspectives on sustainable approaches to fungal disease management in agriculture.

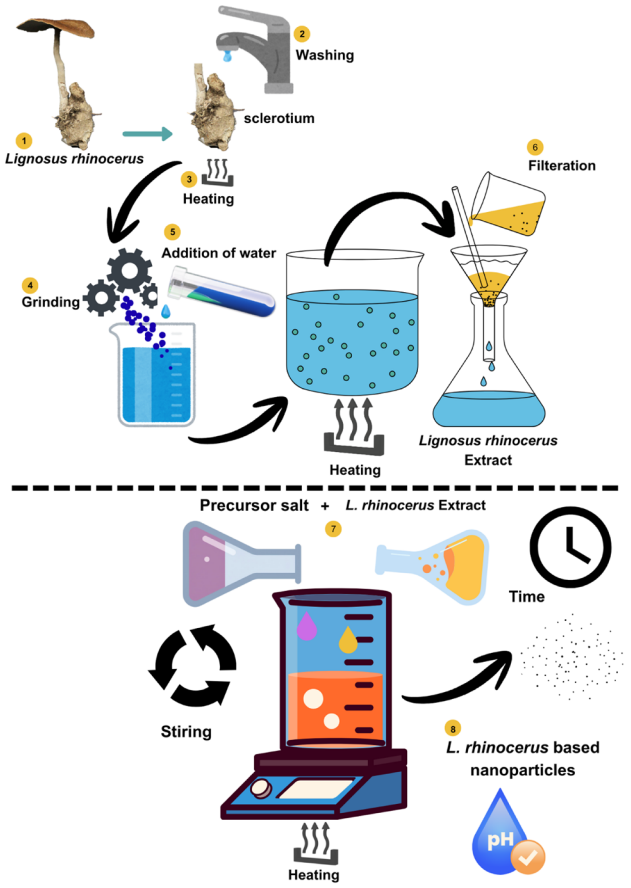

Fig. 1 Overview of *Lignosus rhinocerus*-based silver nanoparticles (LR-AgNPs) from mushroom extract

Materials and methods

Collection of *L. rhinocerus* material and extract preparation

Fruiting bodies of *L. rhinocerus* were obtained from the Institute for Tropical Biology and Conservation (ITBC), Universiti Malaysia Sabah. The fruiting bodies were thoroughly washed three times with distilled water to remove impurities it was then dried in a dehydrator for 3 days and powdered using a domestic miller (MX-GX1521; Panasonic, Tokyo, Japan). Twenty grams of the mushroom powder was added into 200 ml of distilled water and boiled for 10 min. After that, it was filtered through Whatman No. 1 filter paper, and the resulting mushroom extract was collected and kept in the refrigerator at 4 °C (Faris Taufeq et al. 2025; Eskandari-Nojehdehi et al. 2016).

Synthesis of silver nanoparticles

For LR-AgNPs biosynthesis, an aqueous silver nitrate ($AgNO_3$) solution and aqueous mushroom extract was prepared to reduce Ag^+ to Ag^0 to produce AgNPs. 1.699 g of $AgNO_3$ was dissolved in 100 mL of distilled water to prepare a 0.1 M silver nitrate solution. To initiate biosynthesis, 10 mL of aqueous mushroom extract was added to 90 mL of a silver nitrate solution (0.1 M). This mixture was then mixed well and incubated in a rotary shaker incubator overnight at an agitation speed of 150 rpm in the dark at room temperature (Fig. 1). A negative control consisted of mushroom extract without silver nitrate solution. The mushroom extract color changed from light green to brown, indicating the formation of AgNPs. The synthesized nanoparticles were subsequently washed with distilled water prior to further characterization and antifungal assays (Amr et al. 2023; Khan et al. 2023).

Characterizations of *Lignosus rhinocerus* based silver nanoparticles (LR-AgNPs)

The optical stability of LR-AgNPs was analysed by measuring the absorbance using a UV–Vis spectrophotometer (JASCO Corp., V-570 USA) at a wavelength range of 200–800 nm. The surface images of nanoparticles were obtained

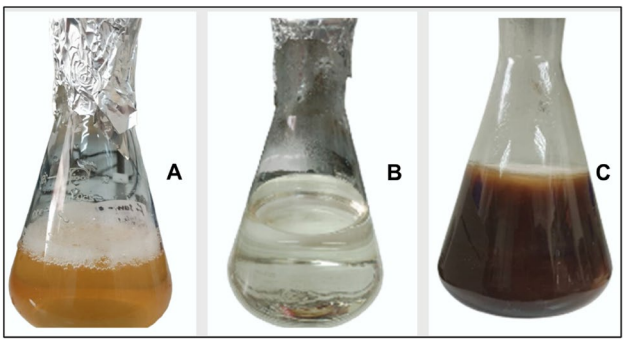

Fig. 2 The apparent changes during biosynthesis of silver nanoparticles utilising *L. rhinocerus* extract. **A** The initial *L. rhinocerus* exhibiting light-brown color. **B** The transparent silver nitrate solution before mixing with extract. **C** The final reaction mixture, upon heating, exhibits a dark-brown color, is the indication of reduction of silver ions into silver nanoparticles

using a scanning electron microscope (SEM) coupled with energy-dispersive X-ray spectroscopy (EDX) (Sarkar et al. 2024). The infra-red analysis of the LR-AgNPs samples was done on a FTIR (Bruker VERTEX 80, Germany), in the wavenumber range of 4000–400 cm^{-1}, with resolution 4 cm^{-1}, refractive index 2.4 (Mehrdel et al. 2023). The particle size distribution of *Lignosus rhinocerus*-mediated silver nanoparticles (LR-AgNPs) was determined using dynamic light scattering (DLS). The nanoparticle suspension was diluted with deionized water and analyzed at 25 °C. The hydrodynamic diameter and polydispersity index (PDI) were calculated based on Brownian motion, and measurements were performed in triplicate to ensure accuracy (Li et al. 2024; Ivanova et al. 2024).

Test fungal pathogens

Fusarium solani and *Aspergillus ochraceus* were used in this work and were obtained from the culture collection of the Mycology Laboratory, Institute for Tropical Biology and Conservation, Universiti Malaysia Sabah, Malaysia. The fungal pathogens were initially characterized based on their morphological features and preserved on PDA plates and kept at 25 ± 1 °C to obtain actively growing cultures for testing (James et al. 2022; Carolis et al. 2012).

Evaluation of *in vitro* antifungal activity

Well diffusion assay

The well diffusion assay was performed to study the antifungal activity of *L. rhinocerus* mediated silver nanoparticles (LR-AgNPs) with little modifications. The fungal spore suspension (1.5×10^8 conidia mL^{-1}) was thoroughly dispersed on sterile solidified PDA medium (Kora and Arunachalam 2011). Six wells of 5.5 mm diameter were made on each agar plate with the help of a sterile cork-borer. Fluconazole stock was prepared by dissolving 2 mg tablet powder in 2 mL distilled water while nanoparticle stock was made by dispersing 5 mg of LR-AgNPs powder in 5 mL distilled water to obtain an equivalent concentration and then further diluted to their respective concentrations. The wells were filled with 90 µL of different concentrations (100, 200, 300, 400, and 500 ppm) of LR-AgNPs in triplicate. The unit "ppm" refers to total nanoparticle suspension concentration. The plates were incubated at 25 °C for seven days, and the zones of inhibition were measured. Fluconazole with same concentrations (100, 200, 300, 400, and 500 ppm) were used well as a positive control. Sterile distilled water was used as the negative control. Experiment was conducted in triplicate (n = 3). The Petri plates were placed in an incubator for one day at 25 °C for seven days (Logeswari et al. 2015).

Radial growth method

Potato dextrose agar (PDA) medium was prepared containing LR-AgNPs with varying final concentrations (100, 200,

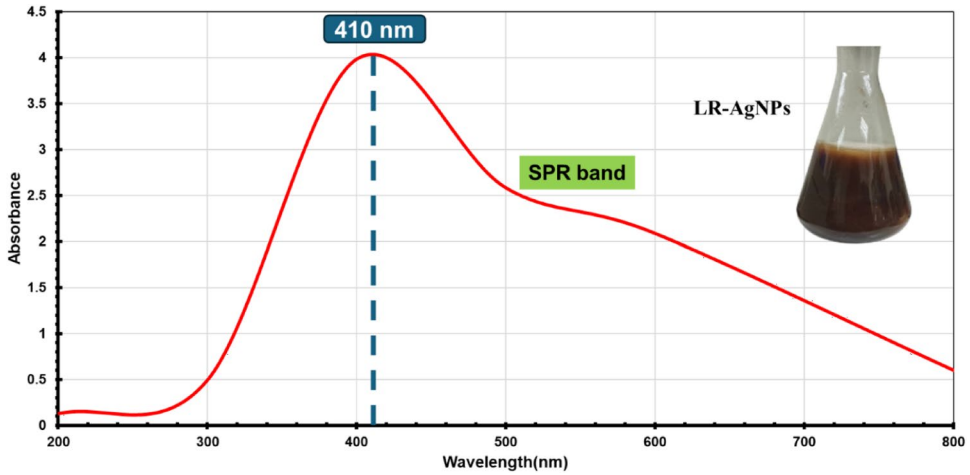

Fig. 3 The UV–Visible absorption spectrum LR-AgNPs possess a strong surface plasmon resonance (SPR) peak at 410 nm that indicates the relatively stable based on UV–Vis, and spherical LR-AgNPs formation

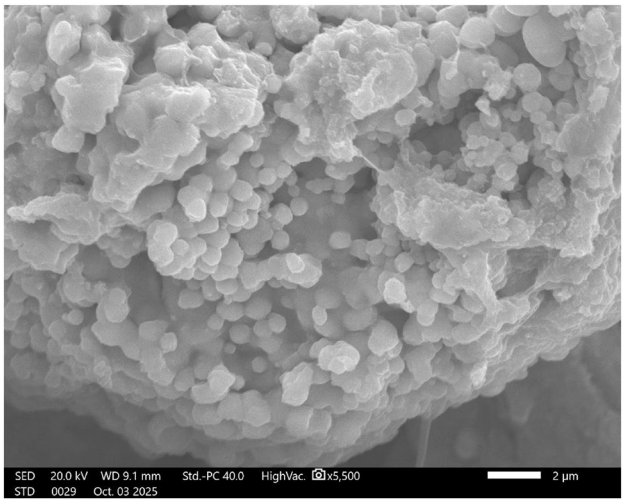

Fig. 4 Scanning electron microscopy (SEM) of *L. rhinocerus* mediated silver nanoparticles (LR-AgNPs). The SEM micrograph obtained at 20.0 kV, wd 9.1, mm, × 5,500 magnification, and a scale bar of 2 µm

300, 400, and 500 ppm) separately. For positive control, no nanoparticles were added. The pathogen was inoculated after the medium had solidified (Bibi et al. 2023). Experiment was conducted in triplicate (n = 3). The inhibition percentage of pathogen growth was calculated using the following equation:

$$\text{Inhibition of pathogen growth}\,(\%) = \frac{\text{Growth in control} - \text{Growth in Treatment}}{\text{Growth in control}} \times 100$$

Statistical analysis

All the measured data were statistically analysed using Statistics 8.1. Data was analyzed using one-way ANOVA, followed by Tukey's HSD test at $p \leq 0.05$. All experiments were conducted in triplicate (n = 3) (Shahbaz et al. 2023).

Results

Synthesis and characterizations of *L. rhinocerus* mediated silver nanoparticles (LR-AgNPs)

Lignosus rhinocerus extract was used as the natural agent that facilitated the reaction in the green synthesis of silver nanoparticles (LR-AgNPs). The biosynthetic process began by combining the *Lignosus rhinocerus* extract with the aqueous silver nitrate solution. The reaction mixture initially exhibited a light brown colour followed by a gradual change to dark brown which confirmed confirms the formation of silver nanoparticles (Fig. 2).

The UV–Visible spectrum of the silver nanoparticles synthesized using *Lignosus rhinocerus* extract revealed an absorption peak at 410 nm, which is characteristic of the surface plasmon resonance (SPR) of spherical-shaped silver nanoparticles (Fig. 3).

The SEM analysis of the LR-AgNPs showed that the particles were mostly spherical or slightly irregular and formed dense aggregates. When examined at a higher magnification, each nanoparticle was about 60–85 nm in size (Fig. 4). The particles had a smooth surface with no clear facets, and the presence of aggregations was probably due to sample preparation during the analysis. The nanoparticles size range of 60–85 nm and predominantly spherical morphology were identified.

The effective reduction of Ag^{+} and synthesis of AgNPs were validated by energy-dispersive X-ray spectroscopy (EDX) analysis of LR-AgNPs. The highest silver elemental peak indicated the formation of LR-AgNPs which exhibited 27.21 wt% (or 80.37 wt% normalized and 46.16 at. %). Similarly, small peaks of Iron (Fe), carbon (C), oxygen (O), and aluminium (Al) were also recorded (Fig. 5).

Numerous distinctive peaks provided detailed information on various functional groups in the FTIR analysis (Fig. 6). The peaks at 3225 cm^{-1} corresponded to the

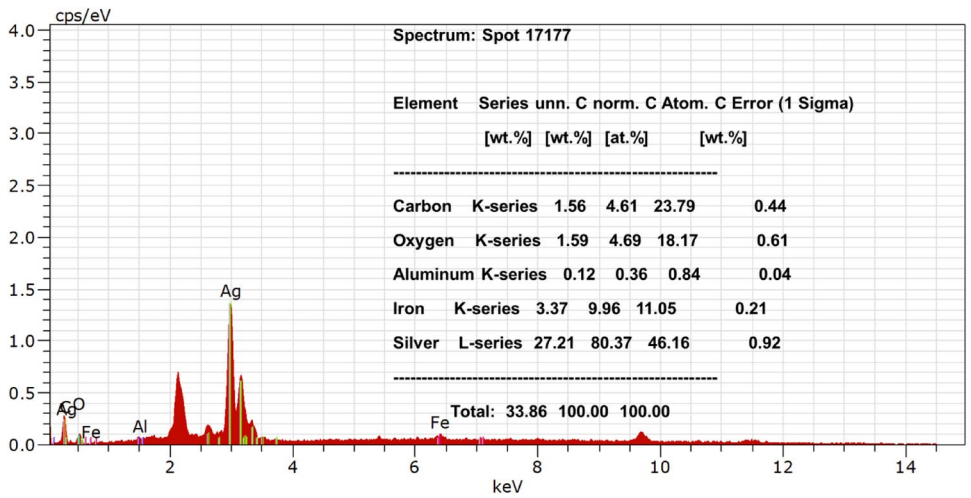

Fig. 5 Energy-dispersive X-ray (EDX) spectrum of biosynthesized silver nanoparticles obtained using *Lignosus rhinocerus* aqueous extract

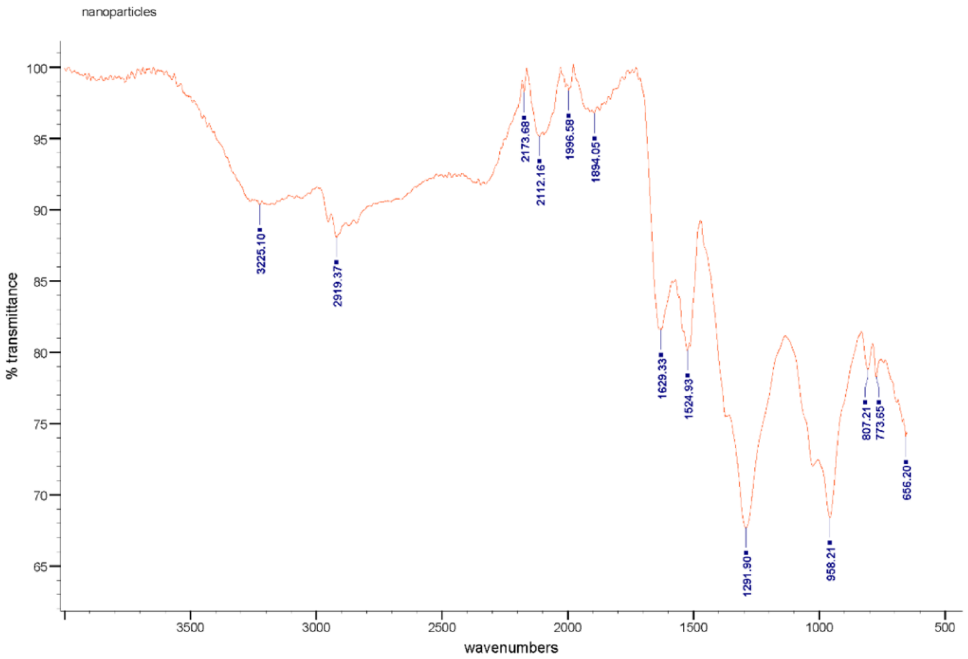

Fig. 6 FTIR spectrum of silver nanoparticles synthesized using *L. rhinocerus* extract

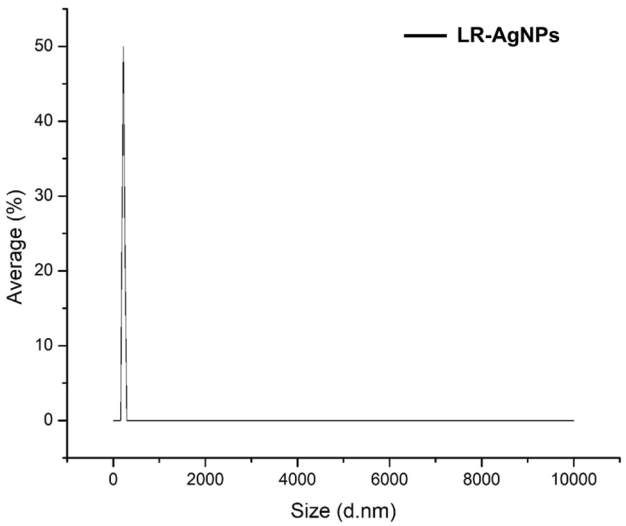

Fig. 7 Dynamic light scattering (DLS) analysis of *Lignosus rhinocerus*-mediated silver nanoparticles (LR-AgNPs) showing particle size distribution

presence of -OH and -NH stretching vibrations, the band at 2918–2773 cm^{-1} represented aliphatic C-H stretching, while the peaks at 1630 cm^{-1} (Amide I) and 1524 cm^{-1} (Amide II) were observed. 1630 cm^{-1} (Amide I) and 1524 cm^{-1} (Amide II), 291 cm^{-1} and in the 958–686 cm^{-1} corresponded region corresponded to C–N, C–O, and C–O–C vibrations.

The dynamic light scattering (DLS) profile of *Lignosus rhinocerus*-mediated silver nanoparticles (LR-AgNPs) shows a particle size distribution with a dominant peak cantered at approximately ~ 100 nm, within a size range of ~ 80–120 nm. The intensity distribution indicates that the majority of nanoparticles are relatively uniform in size, with a sharp and well-defined peak suggesting near monodispersity. The average particle size falls within the nanoscale range, while the absence of multiple broad peaks suggests minimal aggregation. The low polydispersity implied by the sharp distribution indicates good stability of the synthesized nanoparticles in colloidal suspension (Fig. 7).

Antifungal activities

Well diffusion assay

In this study, the antifungal efficacy of *L. rhinocerus* derived silver nanoparticles (LR-AgNPs) was assessed were assessed against *F. solani* and *A. ochraceus* using agar well diffusion assay. The results showed that LR-AgNPs were effective in inhibiting the fungal strains that were tested. The inhibition zones increased with increasing concentrations of LR-AgNPs- For *F. solani*, LR-AgNPs at the concentrations of 100, 200, 300, 400, and 500 ppm produced inhibition zones measuring 13.3, 14.0, 20.0, 25.3, and 33.0 mm, respectively. The inhibition zones for *A. ochraceus* were 9.7, 11.3, 13.0, 14.0, and 16.0 mm. Fluconazole (FLZ), an antifungal drug, was tested under the same concentrations that exhibited inhibition zones of 14.3, 16.7, 18.0, 26.0 and 34.7 mm for *F. solani* at the concentrations of 100, 200, 400 and 500 ppm respectively. The highest inhibitory effect was observed at 500 ppm LR-AgNPs against *F. solani* (33.0 mm), 500 ppm FLZ against *F. solani* (34.7 mm). Similarly, *A. ochraceus* produced inhibition zones of 13.33, 15.34, 13, 14, and 18 mm with the FLZ concentrations 100, 200, 300, 400, and 500 ppm. Maximum inhibition zone was recorded at 500 ppm of FLZ (Figs. 8 and 9).

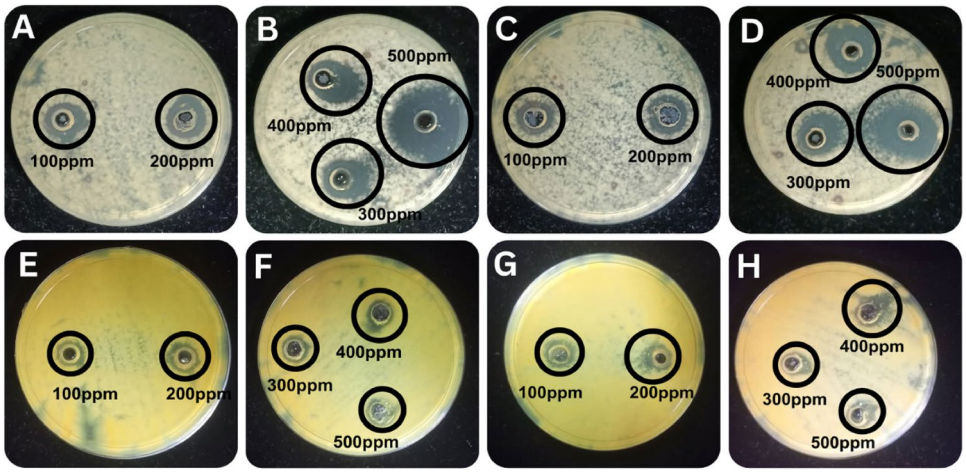

Fig. 8 Antifungal bioassay of *Lignosus rhinocerus* based silver nanoparticles (LR-AgNPs) and antifungal drug (Flucozol) against *Fusarium solani***A** LR-AgNPs (100 and 200), **B** LR-AgNPs (300, 400, and 500), **C** antifungal drug (Flucozol) (100 and 200**), D** antifungal drug (Flucozol) (300, 400, and 500). Antifungal bioassay of *Lignosus rhinocerus* mediated silver nanoparticles (LR-AgNPs) and antifungal drug (Flucozol) against *A. ochraceus***E** LR-AgNPs (100 and 200), **F** LR-AgNPs (300, 400, and 500), **G** antifungal drug (Flucozol) (100 and 200), **H** antifungal drug (Flucozol) (300, 400, and 500)

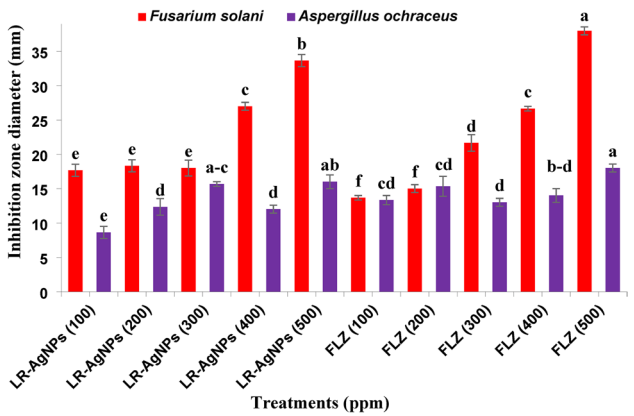

Fig. 9 Concentration-dependent antifungal activity of *Lignosus rhinocerus*–derived silver nanoparticles (LR-AgNPs) against *Fusarium solani* and *Aspergillus ochraceus*, compared with fluconazole (FLZ). Bars represent mean inhibition zone ± standard error (SE) (n = 3). Significant differences among treatments were determined by one-way ANOVA followed by Tukey's HSD test ($p \leq 0.05$), and different letters above the bars indicate statistically significant differences. The negative control showed no antifungal activity and is not presented

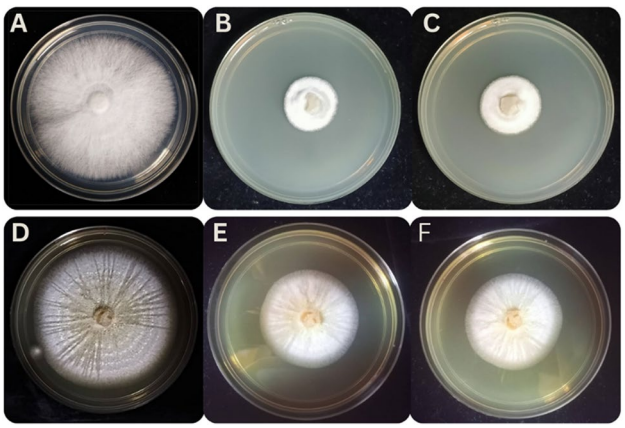

Fig. 10 Antifungal bioassay of *L. rhinocerus* based silver nanoparticles (LR-AgNPs) and antifungal drug (Flucozol) against *F. solani***A** Control (0 ppm) **B** antifungal drug (Flucozol) (500 ppm) **C** LR-AgNPs (500 ppm), **D** Control (0 ppm) **E** antifungal drug (Flucozol) (500 ppm) **F** LR-AgNPs (500 ppm)

The antifungal potential of LR-AgNPs against *F. solani* and *A. ochraceus* was also evaluated using the radial growth method (Fig. 10). The results demonstrated that LR-AgNPs significantly inhibited the mycelial growth of both tested pathogens compared to the untreated control. In the control plates (Fig. 9A), the fungi exhibited unrestricted growth, completely covering the Petri dish surface, with 0% inhibition. In contrast, treatment with fluconazole (FLZ, 500 ppm) markedly suppressed radial growth, producing inhibition levels of 80% for *F. solani* and 66% for *A. ochraceus* (Fig. 10B, C and E, F).

LR-AgNPs at 500 ppm exhibited strong antifungal efficacy, with inhibition values of 76% against *F. solani* and 61% against *A. ochraceus* (Fig. 11), which were slightly lower than those achieved by FLZ but still demonstrated remarkable growth suppression. The reduced colony diameters in the LR-AgNPs–treated plates indicate effective interference with fungal growth and metabolic activity.

Discussion

In current research work, silver nanoparticles were synthesized and their antifungal activities were evaluated against *F. solani* and *A. ochraceus* under laboratory conditions

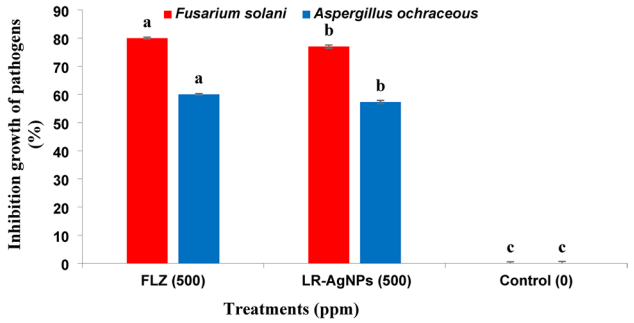

Fig. 11 Inhibition of *Fusarium solani* and *Aspergillus ochraceus* by 500 ppm of *Lignosus rhinocerus*–mediated silver nanoparticles (LR-AgNPs) compared with fluconazole (FLZ). Bars represent mean inhibition zone ± standard error (SE) (n = 3). Significant differences among treatments were determined by one-way ANOVA followed by Tukey's HSD test ($p \leq 0.05$), and different letters above the bars indicate statistically significant differences

using well diffusion and radial growth assays**.** During the synthesis of LR-AgNPs, the reaction mixture first had a light brown colour followed by a gradual change to dark brown that confirms the formation of silver nanoparticles (Aygün et al. 2020). Since the development of a brown color correlates with the surface plasmon resonance associated with silver nanoparticles, this visual alteration was an indication of successful LR-AgNP synthesis (Dal Lago et al. 2011). The silver nitrate solution change from colourless, then light green and finally turns to brown is the indication of silver ions into silver nanoparticles with help of *L. rhinocerus* extract.

Uv–visible spectroscopy was utilized for further confirmation of LR-AgNPs with the presence of a characteristic absorption peak. The sharp, well-defined SPR peak at 410 nm suggested that the nanoparticles formed are relatively small, predominantly spherical and well dispersed. The absence of multiple peaks or significant peak broadening implies minimal aggregation and good stability, likely due to capping by biomolecules from the *L. rhinocerus* extract (Taghavizadeh Yazd et al. 2018). A gradual decline in absorbance beyond the peak, extending into the visible region, further supported the presence of a relatively stable colloid rather than large aggregates or polydisperse particles. The color change to a dark brown solution, as shown in the image, was consistent with silver nanoparticle formation and correlated with the SPR absorption behavior**.** Similar absorption peak was recorded by Saratale et al. (2020). Peng et al. (2013) reported an absorption peak at 415 nm that was closely related to the current study. SPR arises from the collective oscillation of conduction electrons on the nanoparticle surface when excited by light, and its position is strongly influenced by particle size, shape and the dielectric environment (Amin et al.2012).

Scanning electron microscopy (SEM) was applied to know the size and morphology of LR-AgNPs. In current study, nanoparticles possess size of 60–85 nm with spherical morphology. These results are aligned with findings of Verma and Maheshwari (2018), who reported AgNPs size at 79.22 nm. With respect to the observations made in the present study a similar particle size of AgNPs ranging from 55 to 85 nm reported by Mukherjeeet al. (2014). Certain reports have documented extremely smaller particle size in the range 3–18 nm (Sharma et al. 2014) and closely similar size range (30–150 nm) as reported by Sarkar et al. (2011). The nanoparticle size (60–85 nm) likely plays a significant role in antifungal activity, as smaller particles provide a higher surface area that enhances interaction with fungal cells. Additionally, biomolecules present in the *L. rhinocerus* extract may act as capping and stabilizing agents, improving nanoparticle stability and facilitating biological interactions.

Energy Dispersive X-ray Spectroscopy (EDX) was performed to identify the silver as elemental form along with other different elements. These elements act as agent that may be involved in reduction and stabilization of silver cations into silver nanoparticles. Similar elements were reported by Moazzen et al. 2019). The presence of the optical absorbance band at ~ 3 keV, revealed the presence of pure metallic silver nanoparticles (Magudapathy et al. 2001). To identify different functional groups in LR-AgNPs, FTIR analysis was done. These functional group may be involved the reduction of silver cations into silver nanoparticles (Gholamrezazadeh et al. 2023). Our results regarding FTIR are consistent with previous reports (Mohammadi et al. 2019; El-Bendary et al. 2020; Stani et al. 2020). The DLS results indicate that *L. rhinocerus* extract enables the synthesis of relatively uniform silver nanoparticles. The narrow size distribution suggests effective capping and minimal aggregation by bioactive compounds. The observed nanoscale size is suitable for antifungal activity due to enhanced surface area. These findings highlight the potential of *L. rhinocerus* as a green nanofactory, although further analyses such as zeta potential are needed to confirm stability (Ferrari et al. 2024).

In both bioassay evaluations, the agar well diffusion and radial growth assays, LR-AgNPs exhibited concentration dependent increment of antifungal activities. This trend is consistent with the previous studies indicating that the antifungal efficacy of meta nanoparticles is closely correlated with their dosage, as higher concentrations produced more active particles that can interact with fungal cell structures (Singh et al. 2016; Attia 2025). The well diffusion assay showed that LR-AgNPs performed better against *F. solani* than *A. ochraceus*. This disparity in sensitivity may result from differences in cell wall composition, membrane

permeability, and metabolic pathways between two fungi that affect the nanoparticles penetrations and interactions with intracellular targets (Kim et al. 2012). However, it should be considered that the well diffusion method may not fully represent the efficacy of nanoparticles due to their limited diffusion capacity in agar media, which could underestimate their actual antifungal potential. At 500 ppm, LR-AgNPs formed an inhibition zone of 33.0 mm against *F. solani* that was almost the same as fluconazole produced i.e. 34.7 mm. This showed that LR-AgNPs can work as antifungal agents in the same way that a regular antifungal drug does. Fluconazole was used as a standard antifungal reference for comparative purposes; however, it is primarily a clinical antifungal agent and is not commonly applied in plant disease management systems. The radial growth assay confirmed that LR-AgNPs were effective in inhibiting the fungi screened. Fluconazole had slightly higher inhibition potential (80% and 66% respectively), but the fact that LR-AgNPs worked just as well is important because nanoparticles work in different ways than traditional antifungal drugs (Fisher et al. 2018).

Silver nanoparticles are known to generate reactive oxygen species (ROS), compromise membrane integrity, disrupt enzymatic functions and hinder DNA replication in fungal cells (Durán and Marcato 2013; Dakal et al. 2016). The production of ROS is associated with oxidative stress induction that causes lipid peroxidation, dysfunction of mitochondria, and denaturation of proteins that lead towards fungal cell death (Gonzalez-Jimenez et al. 2023) Additionally, nanoparticles have ability to interact directly with fungal cell walls and membranes that enhance the leakage of intracellular contents and metal ions from nanoparticles cause the inhibition of enzymic activities and impair nucleic acid synthesis (Rai et al. 2021; Chen et al. 2020). Silver nanoparticles exert antifungal activity through multiple mechanisms, including disruption of cell membrane integrity, generation of reactive oxygen species (ROS), release of Ag^{+} ions, and interaction with intracellular components such as proteins and DNA. These interactions increase membrane permeability, leading to leakage of cellular contents and inhibition of essential enzymatic processes. Although these mechanisms were not directly investigated in the present study, the observed antifungal activity is likely associated with these well-established modes of action reported in previous studies (Wu et al. 2025; Nasiri-Jahrodi et al. 2024; Irshad et al. 2024).

Consistent with these mechanistic insights, previous reports described the antifungal potential of nanoparticles against *F. solani*. Khatami et al. (2019) applied CuONPs and 80% *F. solani* growth was inhibited at the concentration of 80 µg/mL. Similarly, Chouhan et al. (2022) reported that application of NiCNC showed reduction in rot disease incidence caused by *F. solani* by 83.33% of wheat seedlings. Application of CuNPs showed 61–66% *F. solani* control (Mahawar et al. 2019). Macrocyclic-Amphiphile-Based Self-Assembled Nanoparticles (MASN) nanoparticles were potentially effective against root rot caused by *F. solani* (Shenashen et al. 2017). Peng et al. (2022) reported that SiNPs-induced tolerance to postharvest deterioration and resistance to disease ginger associated with *F. solani*. El-Abeid et al. (2024) applied CuO-Zs-NPs against root rot disease in tomato caused by *F. solani*. Application of these nanoparticles to control Between 72.0 to 88.6% compared to 80.5% disease severity in the infected control. The biosynthesized AgNPs showed strong antifungal activity against *Aspergillus* species. At 500 µg/mL, the inhibition zones were 16 mm (*A. niger*), 20 mm (*A. terreus*), 26 mm (*A. flavus*), and 19 mm (*A. fumigatus*). The MIC values were 125 µg/mL (*A. niger*), 62.5 µg/mL (*A. terreus*), 15.62 µg/mL (*A. flavus*), and 62.5 µg/mL (*A. fumigatus*) (Hashem et al. 2022). The potential of AgNPs to interact with fungal cell wall and interfere with critical physiological functions reflects the significant feature for the fungal disease management. These findings indicate that nanoparticles mediated fungal management is predominantly may be involved by the induction of oxidative stress, membrane damage, and metabolic pathways disruption. These findings suggest that LR-AgNPs could be applied in plant disease management strategies, such as seed treatments, foliar sprays, or soil amendments to reduce fungal infections. These findings highlight the versatile potential of LR-AgNPs in plant disease management. For example, they could be applied as seed treatments, foliar sprays, or soil amendments to reduce fungal infections. In seed treatments, their efficacy can be optimized through nanopriming to activate defense-related enzymes and improve seedling vigor (Luszczyńska et al. 2024). Additionally, seed coating technologies often incorporate polymeric binders, such as Carboxy Methyl Cellulose (CMC) or chitosan, to ensure uniform adhesion to the seed surface and facilitate a controlled release of the active particles during germination (Roopashree et al. 2023). In foliar applications, AgNPs have demonstrated effective reduction of viral and fungal symptoms when applied as a direct spray (Berahmand et al. 2025). The integration of surfactants such as Tween-20 or biological saponins and stickers would be able to reduce surface tension and overcome the hydrophobic nature of leaf cuticles, thus enhancing droplet retention and stomatal penetration (Peirce et al. 2019). This allows the AgNPs to directly inhibit pathogens or trigger induced systemic resistance (ISR) within the plant tissues. Whereas, as soil amendments, LR-AgNPs can be formulated with nanocarriers or stabilizers such as chitosan, polyethylene glycol (PEG), or nanoclays to prevent agglomeration in complex soil environments and ensure targeted delivery to the rhizosphere (Zhang et al. 2023; Zhao et al.

2023; Moore-Neibel et al. 2012). However, further studies under greenhouse and field conditions are necessary to evaluate their effectiveness, stability under environmental conditions, and long-term impact on plant growth.

The limitation of the present study is the absence of appropriate controls, such as $AgNO_3$ alone and *L. rhinocerus* extract alone, which could independently contribute to antifungal activity. Inclusion of these controls in future studies would allow clearer differentiation of the specific effects of synthesized nanoparticles. Therefore, LR-AgNPs in current study demonstrated an efficient strategy alternative to traditional fungicides for controlling plant fungal diseases, with strong potential for application in sustainable plant disease management and crop protection systems.

Conclusions

The study illustrated that *L. rhinocerus* extract served as an effective biological medium for the synthesis of silver nanoparticles with promising antifungal activities. The LR-AgNPs were successfully synthesized using a green method with well-defined shape and size characteristics. Different concentrations of LR-AgNPs inhibited the fungus *F. solani* and *A. ochraceus* indicating their potential as an eco-friendly antifungal agent. Further research into their mechanism of action, biosafety, and field-based formulations will be crucial for the advancement of LR-AgNPs towards real-world applications.

Acknowledgements The authors are gratefully acknowledging the Postgraduate Research Grant (UMSGREAT: GUG0659-2/2023) to (M.S), and the LPK2212 grant to (J.S.S.S), which funded the field and laboratory work. We also appreciate the assistance of the Sabah Forestry Department and Yayasan Sabah and extend our gratitude to the Sabah Biodiversity Center (SaBC) for issuing the sample collection permits (JKM/MBS.1000-2/2 JLD.20 (146) for (M.S) and (JKM/MBS.1000-2/2 JLD.11(2) for (C.C.C).

Author contributions Conceptualization and data curation: Muhammad Shahbaz and Jaya Seelan Sathiya Seelan. Formal analysis: Muhammad Shahbaz and Chong Chuan Cheak. Funding acquisition: Jaya Seelan Sathiya Seelan. Investigation: Jaya Seelan Sathiya Seelan. Methodology: Muhammad Shahbaz, Chong Chuan Cheak and Jaya Seelan Sathiya Seelan. Project administration: Jaya Seelan Sathiya Seelan. Resources: Jaya Seelan Sathiya Seelan and Kishneth Palaniveloo. Supervision: Jaya Seelan Sathiya Seelan. Validation: Jaya Seelan Sathiya Seelan and Kishneth Palaniveloo. Writing—original draft: Muhammad Shahbaz and Chong Chuan Cheak. Writing—review & editing: Muhammad Shahbaz, Chong Chuan Cheak, Kishneth Palaniveloo and Jaya Seelan Sathiya Seelan.

Funding This research was supported by Postgraduate Research Grant (UMSGREAT: GUG0659-2/2023), and LPK2212 grant.

Data availability All relevant data are within the manuscript.

Declarations

Conflict of interest The authors have declared that no competing interests exist.

References

Amr M, Abu-Hussien SH, Ismail R, Aboubakr A, Wael R, Yasser M, Abd-Elhalim BT (2023) Utilization of biosynthesized silver nanoparticles from *Agaricus bisporus* extract for food safety application: Synthesis, characterization, antimicrobial efficacy, and toxicological assessment. Sci Rep 13(1):15048

Attia EA (2025) Mycosynthesis, characterization, antimicrobial and antitumor activity of silver nanoparticles using endophytic *Trichoderma harzianum* isolated from macroalgae *Ulva lactuca*. Egypt Acad J Biol Sci G Microbiol 17(1):27–52

Aygün A, Özdemir S, Gülcan M, Cellat K, Şen F (2020) Synthesis and characterization of Reishi mushroom-mediated green synthesis of silver nanoparticles for the biochemical applications. J Pharm Biomed Anal 178:112970

Azlan AYH, Katas H, Jalluddin NQ, Mh Busra MF (2020) Gold nanoparticles biosynthesized using *Lignosus rhinocerotis* extracts: Comparative evaluation of biostatic and cytotoxicity effects. Sains Malaysiana 49(7):1697–1712

Beltrán Pineda ME, Lizarazo Forero LM, Sierra YCA (2023) Mycosynthesis of silver nanoparticles: a review. Biometals 36(4):745–776

Berahmand A et al (2025) Silver nanoparticles help plants grow, alleviate stresses, and fight pathogens. Plants 14(3):428

Bibi S, Raza M, Shahbaz M, Ajmal M, Mehak A, Fatima N, Maimaiti Y (2023) Biosynthesized silver nanoparticles enhanced wheat resistance to *Bipolaris sorokiniana*. Plant Physiol Biochem 203:108067

Blakeney M (2022) Agricultural innovation and sustainable development. Sustainability 14(5):2698

Cai W, Hu T, Bakry AM, Zheng Z, Xiao Y, Huang Q (2018) Effect of ultrasound on size, morphology, stability and antioxidant activity of selenium nanoparticles dispersed by a hyperbranched polysaccharide from *Lignosus rhinocerotis*. Ultrason Sonochem 42:823–831

Chen J, Wu L, Lu M, Lu S, Li Z, Ding W (2020) Comparative study on the fungicidal activity of metallic MgO nanoparticles and macroscale MgO against soilborne fungal phytopathogens. Front Microbiol 11:365

Chen C, Ma M, Liu G, Ma F, Bao Z (2025) The fungal pathogen *Fusarium solani* poses an increasing threat to tomato production in Northern China. N Z J Crop Hortic Sci 53(4):855–869

Chouhan D, Dutta A, Kumar A, Mandal P, Choudhuri C (2022) Application of nickel chitosan nanoconjugate as an antifungal agent for combating *Fusarium* rot of wheat. Sci Rep 12(1):14518

Dakal TC, Kumar A, Majumdar RS, Yadav V (2016) Mechanistic basis of antimicrobial actions of silver nanoparticles. Front Microbiol 7:1831

Dal Lago V, de Oliveira LF, de Almeida Gonçalves K, Kobarg J, Cardoso MB (2011) Size-selective silver nanoparticles: future of biomedical devices with enhanced bactericidal properties. J Mater Chem 21(33):12267–12273

De Carolis E, Posteraro B, Lass-Flörl C, Vella A, Florio AR, Torelli R, Fadda G (2012) Species identification of Aspergillus, Fusarium and Mucorales with direct surface analysis by matrix-assisted laser desorption ionization time-of-flight mass spectrometry. Clin Microbiol Infect 18(5):475–484

Dean R, Van Kan JA, Pretorius ZA, Hammond-Kosack KE, Di Pietro A, Spanu PD, Foster GD (2012) The Top 10 fungal pathogens in molecular plant pathology. Mol Plant Pathol 13(4):414–430

Desai S, Dubey SC, Prasad RD (2020) Impacts of climate change on *Fusarium* species vis-à-vis adaptation strategies. Indian Phytopathol 73(4):593–603

Durán N, Marcato PD (2013) Nanobiotechnology perspectives. Role of nanotechnology in the food industry: a review. Int J Food Sci Technol 48(6):1127–1134

El-Abeid SE, Mosa MA, El-Tabakh MA, Saleh AM, El-Khateeb MA, Haridy MS (2024) Antifungal activity of copper oxide nanoparticles derived from *Zizyphus spina* leaf extract against *Fusarium* root rot disease in tomato plants. Journal of Nanobiotechnology 22(1):28

El-Bendary MA, Moharam ME, Abdelraof M, Allam MA, Roshdy AM, Shaheen MN, Elkomy GM (2020) Multi-bioactive silver nanoparticles synthesized using mosquitocidal *Bacilli* and their characterization. Arch Microbiol 202(1):63–75

Eskandari-Nojehdehi M, Jafarizadeh-Malmiri H, Rahbar-Shahrouzi J (2016) Optimization of processing parameters in green synthesis of gold nanoparticles using microwave and edible mushroom (*Agaricus bisporus*) extract and evaluation of their antibacterial activity. Nanotechnol Rev 5(6):537–548

Evelyn J (1994) The diary of John Evelyn, 1st edn. Nabu Press, Charleston

Faris Taufeq FY, Nordin ML, Katas H (2025) Upscaling, toxicity and efficacy of multifaceted dressing embedded with dsirna-loaded gold nanoparticles for enhancing diabetic wound treatment. PLoS ONE 20(9):e0327375

Fatima F, Verma SR, Pathak N, Bajpai P (2016) Extracellular mycosynthesis of silver nanoparticles and their microbicidal activity. J Glob Antimicrob Resist 7:88–92

Fernando WG, Miller JD, Seaman WL, Seifert K, Paulitz TC (2000) Daily and seasonal dynamics of airborne spores of *Fusarium graminearum* and other *Fusarium* species sampled over wheat plots. Can J Bot 78(4):497–505

Ferrari GA, Nascimento MA, Bernardo EL, Cortêz MO, Teixeira AV, Oliveira AF, Moreira RP (2024) Development of a selective spectrophotometric method for deltamethrin using silver nanoparticles. Processes 12(9):2041

Fisher MC, Hawkins NJ, Sanglard D, Gurr SJ (2018) Worldwide emergence of resistance to antifungal drugs challenges human health and food security. Science 360(6390):739–742

Fung SY, Yap HYY, Ng ST, Tan CS (2022) In vitro inhibition of melanin formation and enhancement of collagen production by a mushroom sclerotial water extract from the tiger milk mushroom, *Lignosus rhinocerus* (Agaricomycetes), with no skin and eye irritation. Int J Med Mushrooms. https://doi.org/10.1615/intjmedmushrooms.2022043505

Gholamrezazadeh C, Hakimi M, Dadmehr M (2023) A new and safe spirocyclic alkoxy phosphazene: synthesis, characterization, DFT, molecular docking and photophysical properties. Chem Methodol 7(12):944–963

Gonzalez-Jimenez I, Perlin DS, Shor E (2023) Reactive oxidant species induced by antifungal drugs: identity, origins, functions, and connection to stress-induced cell death. Front Cell Infect Microbiol 13:1276406

Hagos L, Guta M, Bacha K (2024) Prevalence of mycotoxigenic fungi and ochratoxin A in coffee (*Coffea arabica* L.). Cogent Food Agric 10(1):2407524

Hashem AH, Saied E, Amin BH, Alotibi FO, Al-Askar AA, Arishi AA, Elbahnasawy MA (2022) Antifungal activity of biosynthesized silver nanoparticles (AgNPs) against *aspergilli* causing aspergillosis: ultrastructure study. J Funct Biomater 13(4):242

Irshad MA, Hussain A, Nasim I, Nawaz R, Al-Mutairi AA, Azeem S, Zaki ME (2024) Exploring the antifungal activities of green nanoparticles for sustainable agriculture: a research update. Chem Biol Technol Agric 11(1):133

Ivanova N, Ermenlieva N, Simeonova L, Vilhelmova-Ilieva N, Bratoeva K, Stoyanov G, Andonova V (2024) In situ gelling behavior and biopharmaceutical characterization of nano-silver-loaded poloxamer matrices designed for nasal drug delivery. Gels 10(6):385

James JE, Santhanam J, Zakaria L, Mamat Rusli N, Abu Bakar M, Suetrong S, Cannon RD (2022) Morphology, phenotype, and molecular identification of clinical and environmental *Fusarium solani* species complex isolates from Malaysia. J Fungi 8(8):845

Johnathan M, Gan SH, Ezumi MW, Faezahtul AH, Nurul AA (2016) Phytochemical profiles and inhibitory effects of Tiger Milk mushroom (*Lignosus rhinocerus*) extract on ovalbumin-induced airway inflammation in a rodent model of asthma. BMC Complement Altern Med 16(1):167

Katas H, Lim CS, Azlan AYHN, Buang F, Busra MFM (2019) Antibacterial activity of biosynthesized gold nanoparticles using biomolecules from *Lignosus rhinocerotis* and chitosan. Saudi Pharm J 27(2):283–292

Khan S, Fiaz M, Yasmin H, Ahmad J, Ullah A, Niaz Z, Farid A (2023) Molecular profiling, characterization and antimicrobial efficacy of silver nanoparticles synthesized from *Calvatia gigantea* and *Mycena leaiana* against multidrug-resistant pathogens. Molecules 28(17):6291

Khatami M, Varma RS, Heydari M, Peydayesh M, Sedighi A, Agha Askari H, Khatami S (2019) Copper oxide nanoparticles greener synthesis using tea and its antifungal efficiency on *Fusarium solani*. Geomicrobiol J 36(9):777–781

Kim SW, Jung JH, Lamsal K, Kim YS, Min JS, Lee YS (2012) Antifungal effects of silver nanoparticles (AgNPs) against various plant pathogenic fungi. Mycobiology 40(1):53–58

Kora AJ, Arunachalam J (2011) Assessment of antibacterial activity of silver nanoparticles on *Pseudomonas aeruginosa* and its mechanism of action. World J Microbiol Biotechnol 27:1209–1216

Lau BF, Abdullah N, Aminudin N, Lee HB, Yap KC, Sabaratnam V (2014) The potential of mycelium and culture broth of *Lignosus rhinocerotis* as substitutes for the naturally occurring sclerotium with regard to antioxidant capacity, cytotoxic effect, and low-molecular-weight chemical constituents. PLoS ONE 9(7):e102509

Lee SS, Tan NH, Fung SY, Pailoor J, Sim SM (2011) Evaluation of the sub-acute toxicity of the sclerotium of *Lignosus rhinocerus* (Cooke), the Tiger Milk mushroom. J Ethnopharmacol 138(1):192–200

Lee SS, Tan NH, Fung SY, Sim SM, Tan CS, Ng ST (2014) Anti-inflammatory effect of the sclerotium of *Lignosus rhinocerotis* (Cooke) Ryvarden, the Tiger Milk mushroom. BMC Complement Altern Med 14(1):359

Amin, M., Anwar, F., Janjua, M. R. S. A., Iqbal, M. A., & Rashid, U. (2012). Green synthesis of silver nanoparticles through reduction with Solanum xanthocarpum L. berry extract: characterization, antimicrobial and urease inhibitory activities against Helicobacter pylori. International journal of molecular sciences, 13(8), 9923-9941.

Li PJ, Xie RS, Pan JJ, Jiang YQ, Liu X (2024) Physicochemical characterization and antibacterial activities of silver nanoparticles prepared by amidated low-methoxyl pectin. RSC Adv 14(52):38582–38589

Logeswari P, Silambarasan S, Abraham J (2015) Synthesis of silver nanoparticles using plants extract and analysis of their antimicrobial property. J Saudi Chem Soc 19(3):311–317

Luszczyńska K et al (2024) Seeds priming with bio-silver nanoparticles protects pea (*Pisum sativum* L.) seedlings against selected fungal pathogens. Int J Mol Sci 25(21):11402

Magudapathy P, Gangopadhyay P, Panigrahi BK, Nair KGM, Dhara S (2001) Electrical transport studies of Ag nanoclusters embedded in glass matrix. Phys B 299(1–2):142–146

Mahawar H, Prasanna R, Gogoi R (2019) Elucidating the disease alleviating potential of cyanobacteria, copper nanoparticles and their interactions in *Fusarium solani* challenged tomato plants. Plant Physiol Rep 24(4):533–540

Manimaran K, Yanto DHY, Anita SH, Nurhayat OD, Selvaraj K, Basavarajappa S, Kumarasamy K (2023) Synthesis and characterization of *Hypsizygus ulmarius* extract mediated silver nanoparticles (AgNPs) and test their potentiality on antimicrobial and anticancer effects. Environ Res 235:116671

Mehrdel B, Yehya AHS, Dheyab MA, Jameel MS, Aziz AA, Nikbakht A, Kareem AA (2023) The antibacterial and toxicological studies of mycosynthesis silver nanoparticles by isolated phenols from *agaricus bisporus*. Phys Scr 98(12):125007

Moazzen M, Khaneghah AM, Shariatifar N, Ahmadloo M, Eş I, Baghani AN, Khaniki GJ (2019) Multi-walled carbon nanotubes modified with iron oxide and silver nanoparticles (MWCNT-Fe3O4/Ag) as a novel adsorbent for determining PAEs in carbonated soft drinks using magnetic SPE-GC/MS method. Arab J Chem 12(4):476–488

Mohammadi M, Shahisaraee SA, Tavajjohi A, Pournoori N, Muhammadnejad S, Mohammadi SR, Delavari H H (2019) Green synthesis of silver nanoparticles using *Zingiber officinale* and *Thymus vulgaris* extracts: characterisation, cell cytotoxicity, and its antifungal activity against *Candida albicans* in comparison to fluconazole. IET Nanobiotechnol 13(2):114–119

Kamal, N., Adnan, H., & Latip, J. (2023). Phytochemical screening and antibacterial activity of *Lignosus rhinocerotis* (Cooke) ryvarden grown in open field and indoor. Gazi University Journal of Science, 36(4), 1496-1504

Moore-Neibel K, Gerber C, Patel J, Friedman M, Ravishankar S (2012) Antimicrobial activity of lemongrass oil against *Salmonella enterica* on organic leafy greens. J Appl Microbiol 112(3):485–492

Mukherjee S, Chowdhury D, Kotcherlakota R, Patra S, Bhadra MP, Sreedhar B, Patra CR (2014) Potential theranostics application of bio-synthesized silver nanoparticles (4-in-1 system). Theranostics 4(3):316

Nasiri-Jahrodi A, Shams-Ghahfarokhi M, Paskiabi FA, Razzaghi-Abyaneh M (2024) Unraveling the mechanism of antifungal action of encapsulated eugenol/chitosan nanoparticles against *Aspergillus fumigatus*. J Drug Deliv Sci Technol 95:105595

Nizamani MM, Hughes AC, Zhang HL, Wang Y (2024) Revolutionizing agriculture with nanotechnology: innovative approaches in fungal disease management and plant health monitoring. Sci Total Environ. https://doi.org/10.1016/j.scitotenv.2024.172473

O'Donnell K, Ward TJ, Robert VA, Crous PW, Geiser DM, Kang S (2015) DNA sequence-based identification of *Fusarium*: current status and future directions. Phytoparasitica 43:583–595

Peirce CA, McBeath TM, Priest C, McLaughlin MJ (2019) The timing of application and inclusion of a surfactant are important for absorption and translocation of foliar phosphoric acid by wheat leaves. Front Plant Sci 10:1532

Peng H, Yang A, Xiong J (2013) Green, microwave-assisted synthesis of silver nanoparticles using bamboo hemicelluloses and glucose in an aqueous medium. Carbohyd Polym 91(1):348–355

Peng H, Hu H, Xi K, Zhu X, Zhou J, Yin J, Zhu Y (2022) Silicon nanoparticles enhance ginger rhizomes tolerance to postharvest deterioration and resistance to *Fusarium solani*. Front Plant Sci 13:816143

Perfect SE, Green JR (2001) Infection structures of biotrophic and hemibiotrophic fungal plant pathogens. Mol Plant Pathol 2(2):101–108

Rai M, Bonde S, Golinska P, Trzcińska-Wencel J, Gade A, Abd-Elsalam KA, Ingle AP (2021) *Fusarium* as a novel fungus for the synthesis of nanoparticles: mechanism and applications. J Fungi 7(2):139

Roopashree M et al (2023) Validating protocol and deciphering the nanoparticulate CMC coating in seeds. Int J Plant Soil Sci 35(6):97–105

Saratale GD, Saratale RG, Ghodake G, Shinde S, Kim DY, Alyousef AA, Shin HS (2020) Chlortetracycline-functionalized silver nanoparticles as a colorimetric probe for aminoglycosides: ultrasensitive determination of kanamycin and streptomycin. Nanomaterials 10(5):997

Sarkar J, Dey P, Saha S, Acharya K (2011) Mycosynthesis of selenium nanoparticles. Micro Nano Lett 6(8):599–602

Sarkar J, Naskar A, Nath A, Gangopadhyay B, Tarafdar E, Das D, Acharya K (2024) Innovative utilization of harvested mushroom substrate for green synthesis of silver nanoparticles: a multi-response optimization approach. Environ Res 248:118297

Sharma G, Sharma AR, Bhavesh R, Park J, ET, et al (2014) Biomolecule mediated synthesis of selenium nanoparticles using dried *Vitis vinifera* (Raisin) extract. Molecules 19:2761–70

Shenashen M, Derbalah A, Hamza A, Mohamed A, El Safty S (2017) Recent trend in controlling root rot disease of tomato caused by *Fusarium solani* using aluminasilica nanoparticles. Int J Adv Res Biol Sci 4(6):105–119

Singh P, Kim YJ, Zhang D, Yang DC (2016) Biological synthesis of nanoparticles from plants and microorganisms. Trends Biotechnol 34(7):588–599

Šišić A, Baćanović-Šišić J, Schmidt H, Finckh MR (2025) Effect of management system and pedoclimatic factors on *Fusarium* and *Didymella* communities associated with pea (*Pisum sativum*) roots in Germany. Sci Rep 15(1):2653

Stani C, Vaccari L, Mitri E, Birarda G (2020) FTIR investigation of the secondary structure of type I collagen: New insight into the amide III band. Spectrochim Acta Part A Mol Biomol Spectrosc 229:118006

Summerell BA, Salleh B, Leslie JF (2003) A utilitarian approach to *Fusarium* identification. Plant Dis 87(2):117–128

Taghavizadeh Yazdi ME, Khara J, Sadeghnia HR, Esmaeilzadeh Bahabadi S, Darroudi M (2018) Biosynthesis, characterization, and antibacterial activity of silver nanoparticles using *Rheum turkestanicum* shoots extract. Res Chem Intermed 44(2):1325–1334

Tian B, Xie J, Fu Y, Cheng J, Li BO, Chen T, Jiang D (2020) A cosmopolitan fungal pathogen of dicots adopts an endophytic lifestyle on cereal crops and protects them from major fungal diseases. ISME J 14(12):3120–3135

Tiwari RK, Lal MK, Kumar R, Mangal V, Kumar A, Kumar R, Singh B (2024) Salt stress influences the proliferation of *Fusarium solani* and enhances the severity of wilt disease in potato. Heliyon 10(4)

Tripathi AN, Maurya S, Pandey KK, Behera TK (2024) Global scenario of vegetable fungal diseases. Veg Sci 51:54–65

Verma P, Maheshwari SK (2018) Preparation of sliver and selenium nanoparticles and its characterization by dynamic light scattering and scanning electron microscopy. J Microsc Ultrastruct 6(4):182–187

Waghmode HU, Samudra SM (2025) Biochemical Analysis of Healthy and Infected Soybean Plants with *Fusarium solani* and *Fusarium oxysporum*. Sciences 2(5):155–161

Wong KH, Lai CK, Cheung PC (2011) Immunomodulatory activities of mushroom sclerotial polysaccharides. Food Hydrocolloids 25(2):150–158

Wu Q, Cen F, Xie Y, Ning X, Wang J, Lin Z, Huang J (2025) Nanoparticle-based antifungal therapies innovations mechanisms and future prospects. PeerJ 13:e19199

Zhang X, McKee MS, Filser J (2023) Long-term effects of silver nanoparticles (NM-300K) and soil amendments on soil respiration and mesofauna in a semi-field experiment. Environ Sci Nano 10(8):2090–2101

Zhou F, Peterson T, Fan Z, Wang S (2023) The commonly used stabilizers for phytochemical-based nanoparticles: stabilization effects, mechanisms, and applications. Nutrients 15(18):3881

Shahbaz M, Akram A, Raja NI, Mukhtar T, Mehak A, Fatima N, Abasi F (2023) Antifungal activity of green synthesized selenium nanoparticles and their effect on physiological, biochemical, and antioxidant defense system of mango under mango malformation disease. PLoS One 18(2):e0274679

Sharma G, Sharma AR, Bhavesh R, Park J, Ganbold B, Nam JS, Lee SS (2014) Biomolecule-mediated synthesis of selenium nanoparticles using dried Vitis vinifera (raisin) extract. Mol 19(3):2761-2770

Li, J., Gu, F., Wu, R., Yang, J., & Zhang, K. Q. (2017). Phylogenomic evolutionary surveys of subtilase superfamily genes in fungi. Scientific reports, 7(1), 45456.